

# **Experimental Investigation on the Performance and Efficiency Optimization of a Ranque–Hilsch Vortex Tube for Industrial Applications.**



**A thesis**

**by**

**Md. Asikur Rahman**

**Rafiqul Islam**

**Md. Maruf Hasan**

**Md. Mushfikur Rahman**

**Razia Sultana**

**Submitted to the**

**DEPARTMENT OF MECHANICAL ENGINEERING**

**SONARGAON UNIVERSITY (SU)**

**May 2026**

# **Experimental Investigation on the Performance and Efficiency Optimization of a Ranque–Hilsch Vortex Tube for Industrial Applications.**

**A thesis**

**by**

<b>Md. Asikur Rahman</b>	<b>ME2203028194</b>
<b>Rafiqul Islam</b>	<b>ME2203028019</b>
<b>Md. Maruf Hasan</b>	<b>ME2202027136</b>
<b>Md. Mushfikur Rahman</b>	<b>ME2203028350</b>
<b>Razia Sultana</b>	<b>ME2203028382</b>

**Supervisor: Md. Misbah Uddin**

**Lecturer**

**Submitted to the**

**DEPARTMENT OF MECHANICAL ENGINEERING**

**SONARGAON UNIVERSITY (SU)**

**In partial fulfillment of the requirements for the award of the degree**

**of**

**BACHELOR OF SCIENCE IN MECHANICAL ENGINEERING**

**May 2026**

## DECLARATION

We do hereby solemnly declare that the work presented in this project, the report, has been carried out by us and has not been previously submitted to Any University or Organization for the award of any degree or certificate.

We hereby confirm that the works prevented here do not breach any existing copyright.

We further undertake to indemnify the university against any loss or damage arising from breach of the foregoing obligation.

[Authors]

.....  
**Md. Asikur Rahman**

**ID: ME2203028194**

.....  
**Rafiqul Islam**

**ID: ME2203028019**

.....  
**Md. Maruf Hasan**

**ID: ME2202027136**

.....  
**Md. Mushfikur Rahman**

**ID: ME2203028350**

.....  
**Razia Sultana**

**ID: ME2203028382**

## **ACKNOWLEDGEMENT**

In the name of Almighty Allah, whose blessings enabled the successful completion of this thesis.

The authors would like to express sincere gratitude to **Md. Misbah Uddin, Lecturer, Department of Mechanical Engineering, Sonargaon University**, for his invaluable guidance, constructive feedback, and continuous support throughout this work.

We are also thankful to Professor Md. Mostofa Hossain, Head of the Department of Mechanical Engineering, Sonargaon University, and to all respected faculty members of the department for their kind cooperation and encouragement.

---

**Md. Misbah Uddin**

**Lecturer**

**DEPARTMENT OF MECHANICAL ENGINEERING**

## Abstract

The Ranque–Hilsch vortex tube (RHVT) is a simple, compact, and mechanically elegant device that separates a compressed gas stream into a hot and a cold fraction without any moving parts, refrigerants, or external energy input beyond the compressed air itself. Despite decades of research, the underlying energy-separation mechanism is still debated, and the device's relatively low thermodynamic efficiency has limited its widespread industrial adoption. In this study, a counter-flow vortex tube was designed, fabricated from stainless steel and mild steel components, and experimentally tested at five inlet pressures ranging from 6 bar to 9.5 bar. The temperatures at the cold outlet, the hot outlet, and the ambient (normal) condition were recorded with a CIE 305 digital thermometer. Key performance parameters—cold temperature drop ( $\Delta T_c$ ), hot temperature rise ( $\Delta T_h$ ), coefficient of performance (COP), and isentropic efficiency—were calculated and analyzed. The results show that the maximum temperature difference of 17.1 °C (between hot and cold streams) was achieved at 9 bar, while the greatest cold-side temperature drop of 15.3 °C below ambient was obtained at the same pressure. A comprehensive graphical data analysis is presented, and recommendations for further efficiency improvements are discussed.

# Table of Contents

<b>DECLARATION</b>	i
<b>ACKNOWLEDGEMENT</b>	ii
<b>ABSTRACT</b>	iii
<b>Chapter -1</b>	
<b>Introduction</b>	1
1.1 Background	1
1.2 Problem Statement	1
1.3 Objectives	2
<b>Chapter -2</b>	
<b>Literature Review</b>	3
<b>Chapter -3</b>	
<b>Experimental Setup and Methodology</b>	11
3.1 Vortex Tube Design and Specifications	11
3.2 Material Selection Rationale	12
3.3 Experimental Procedure	12
3.4 Instruments and Uncertainty	13
<b>Chapter -4</b>	
<b>Experimental Results</b>	14
4.1 Derived Performance Parameters	14
4.2 Isentropic Efficiency Calculation	15
4.3 Coefficient of Performance (COP)	16

## **Chapter -5**

### **Data Analysis and Discussion** 17

5.1 Graphical Data Analysis 17

5.2 Effect of Inlet Pressure on Temperature Separation 21

5.3 Efficiency Analysis 21

5.4 Comparison with Literature 22

5.5 Industrial Applications 22

5.6 Limitation 22

## **Chapter -6**

### **Future Recommendations** 23

## **Chapter -7**

**Conclusions** 24

**References** 25

## List of Figures

Figure 1: Vortex Tube components designed in SolidWorks .....	11
Figure 2: Vortex Tube.....	11
Figure 3: Schematic Diagram of the Experimental Setup .....	13
Figure 4: Temperature Profile vs. Inlet Pressure .....	17
Figure 5: Cold Temperature Drop ( $\Delta T_c$ ) vs. Inlet Pressure.....	18
Figure 6: Total Temperature Separation ( $\Delta T_{total}$ ) vs. Inlet Pressure.....	18
Figure 7: Isentropic Efficiency vs. Inlet Pressure.....	19
Figure 8: COP vs. Inlet Pressure.....	20
Figure 9: Comparison of Hot Rise and Cold Drop at Each Pressure.....	20

## List of Tables

<b>TABLE NAME</b>	<b>PAGE NO</b>
Table 1: Vortex Tube Component Specifications	12
Table 2: Experimental Results	14
Table 3: Derived Temperature Parameters	14
Table 4: Isentropic Efficiency Analysis	15
Table 5: COP of the Vortex Tube (Cold Side)	16

# Chapter-1

## Introduction

### 1.1 Background

The vortex tube was first discovered by the French physicist Georges J. Ranque in 1933 [1] and later improved by the German physicist Rudolf Hilsch in 1947 [2]. The device accepts compressed gas through one or more tangential nozzles, generating a high-speed vortex inside a cylindrical tube. Through a phenomenon that is still the subject of active research—involving combinations of work transfer between concentric vortex layers, acoustic streaming, and secondary circulation—the gas separates into two streams: a cold central stream exiting from one end and a hot peripheral stream exiting from the opposite end.

Because the vortex tube has no moving parts, it offers exceptional reliability, zero maintenance, instant operation, and compact size. These attributes make it attractive for a variety of industrial applications:

Spot cooling of electronic enclosures, control cabinets, and CCTV cameras. Machining operations where cutting-tool cooling is needed without liquid coolants. Gas liquefaction and separation in the petrochemical industry. Personal cooling in hazardous environments where electrical equipment is prohibited. Laboratory temperature control for testing and calibration.

### 1.2 Problem Statement

Although the vortex tube is conceptually simple, its thermodynamic efficiency (typically 20–35 % of isentropic expansion) is considerably lower than that of conventional vapor-compression refrigeration systems. Improving the efficiency or at least identifying the operating point that maximizes temperature separation for a given tube geometry is therefore of practical importance. The present work addresses this by systematically varying the inlet pressure while keeping geometrical parameters fixed, measuring the resulting temperature separation, and computing performance metrics.

### **1.3 Objectives**

To design and fabricate a counter-flow Ranque–Hilsch vortex tube using stainless steel and mild steel.

To experimentally evaluate the temperature separation at different inlet pressures.

To analyze other performance parameters using indicators.

To determine the optimal operating pressure for maximum efficiency.

## Chapter-2

### Literature Review

Ranque (1933) first patented the vortex tube; Hilsch (1947) published the first systematic study and demonstrated improved performance with geometric optimization. Since then, numerous researchers have investigated the effects of various parameters:

Stephan et al. (1983) studied the effect of tube length-to-diameter ratio ( $L/D$ ) and found that ratios of 20–30 provide optimal performance. [3]

Aydın and Baki (2006) explored the influence of the number of nozzles and their geometry, showing that multi-nozzle configurations improve energy separation. [4]

Xue et al. (2010) performed CFD simulations to elucidate the internal flow structure and energy transfer mechanisms. [5]

Thakare and Parekh (2015) reviewed the effects of cold mass fraction, inlet pressure, tube material, and working fluid on vortex tube performance. [6]

Rafiee and Sadeghiazad (2017) examined convergent, straight, and divergent tube geometries and reported that slightly convergent tubes enhance cooling performance. [7]

The consensus in the literature is that inlet pressure is one of the most influential operating parameters; higher pressures generally increase temperature separation up to a saturation point. The present study contributes experimental data from a custom-fabricated tube with specific geometric parameters detailed below.

Vortex flows or swirl flows have been of considerable interest over the past decades because of their use in industrial applications, such as furnaces, gas-turbine combustors and dust collectors. Vortex (or high swirl) can also produce a hot and a cold stream via a vortex tube. The vortex tube has been used in industrial applications for cooling and heating processes because they are simple, compact, light and quiet (in operation) devices [9–20]. Several researchers put a lot of efforts to explain for the phenomena occurring during the energy separation inside the

vortex tube. Research studies about these phenomena were formed mainly into two groups. The first one performed the experimental work (geometrical and thermo-physical parameters) and then through the value of their results attempted to explain the phenomena. The second performed the studies in qualitative, analytical and numerical ways in order to help in the analysis of the mechanisms present in the vortex tube.

The vortex tube was first discovered by Ranque [1,2], a metallurgist and physicist who was granted a French patent for the device in 1932, and a United States patent in 1934. The initial reaction of the scientific and engineering communities to his invention was disbelief and apathy. Since the vortex tube was thermodynamically highly inefficient, it was abandoned for several years. Interest in the device was revived by Hilsch [3], a German engineer, who reported an account of his own comprehensive experimental and theoretical studies aimed at improving the efficiency of the vortex tube. He systematically examined the effect of the inlet pressure and the geometrical parameters of the vortex tube on its performance and presented a possible explanation of the energy separation process. After

Hilsch [3], an experimental study was made by Scheper [23] who measured the velocity, pressure, and total and static temperature gradients in a Ranque–Hilsch vortex tube, using probes and visualization techniques. He concluded that the axial and radial velocity components were much smaller than the tangential velocity. His measurements indicated that the static temperature decreased in a radially outward direction. This result was contrary to most other observations that were made later. Martynovskii and Alekseev [24] studied experimentally the effect of various design parameters of vortex tubes. Hartnett and Eckert [25,26] measured the velocity, total temperature, and total and static pressure distributions inside a uni-flow vortex tube. They used the experimental values of static temperature and pressure to estimate the values of density and hence, the mass and energy flow at

different cross sections in the tube. The results agreed fairly well with the overall mass and energy flow in the tube. Scheller and Brown [27] presented measurements of the pressure, temperature, and velocity profiles in a standard vortex tube and observed that the static temperature decreased radially outwards as in the work of Scheper [23], and hypothesized the energy separation mechanism as heat transfer by forced convection. Blatt and Trusch [28] investigated experimentally the performance of a uniflow vortex tube and improved its performance by adding a radial diffuser to the end of the shortened tube instead of a cone valve. The geometry of the tube was optimised to maximise the temperature difference between the cold and inlet temperatures by changing the various dimensions of the tube such as the gap of the diffuser, tube length, and entrance geometry. Moreover, the effects of inlet pressure and heat fluxes were examined. Linderstrom-Lang [29] studied in detail the application of the vortex tube to gas separation, using different gas mixtures and tube geometry and found that the separation effect depended mainly on the ratio of cold and hot gas mass flow rates. The measurements of Takahama [30] in a counter-flow vortex tube provided data for the design of a standard type vortex tube with a high efficiency of energy separation. He also gave empirical formulae for the profiles of the velocity and temperature of the air flowing through the vortex tube. Takahama and Soga [31] used the same sets of the vortex tubes of Takahama [30] to study the effect of the tube geometry on the energy separation process and that of the cold air flow rate on the velocity and temperature fields for the optimum proportion ratio of the total area of nozzles to the tube area. They also reported an axisymmetric vortex flow in the tube. Vennos [32] measured the velocity, total temperature, and total and static pressures inside a standard vortex tube and reported the existence of substantial radial velocity. Bruun [33] presented the experimental data of pressure, velocity and temperature profiles in a counter-flow vortex tube with a ratio of 0.23 for the

cold to total mass flow rate and concluded that radial and axial convective terms in the equations of motion and energy were equally important. Although no measurements of radial velocities were made, his calculation, based on the equation of continuity, showed an outward directed radial velocity near the inlet nozzle and an inward radial velocity in the rest of the tube. He reported that turbulent heat transport accounted for most of the energy separation. Nash [34] used vortex expansion techniques for high temperature cryogenic cooling to apply to infrared detector applications. A summary of the design parameters of the vortex cooler was reported by Nash [35]. Marshall [36] used several different gas mixtures in a variety of sizes of vortex tubes and confirmed the effect of the gas separation reported by Linderstrom-Lang [29]. A critical inlet Reynolds number was identified at which the separation was a maximum. Takahama et al. [37] investigated experimentally the energy separation performance of a steam-operated standard vortex tube and reported that the performance worsened with wetness of steam at the nozzle outlet because of the effect of evaporation. Energy separation was absent with the dryness fraction less than around 0.98. The measurements of Collins and Lovelace [38] with a two-phase, liquid–vapour mixture, propane in a standard counter-flow vortex tube showed that for an inlet pressure of 0.791 MPa, the separation remained significant for a dryness fraction above 80% at the inlet. With a dryness fraction below 80%, the temperature separation became insignificant. But the discharge enthalpies showed considerable differences indicating that the Ranque–Hilsch process is still in effect. Takahama and Yokosawa [39] examined the possibility of shortening the chamber length of a standard vortex tube by using divergent tubes for the vortex chamber. Earlier researchers such as Parulekar [40], Otten [41], and Raiskii and Tunkel [42] also employed divergent tubes for all or part of the vortex chamber in attempts to shorten the chamber and improve energy separation performance, but their

emphasis was on the maximum and minimum temperatures in the outflowing streams. Therefore, Takahama and Yokosawa [39] compared their results with those from the straight vortex chambers. They found that the uses of a divergent tube with a small angle of divergence led to an improvement in temperature separation and enable the shortening of the chamber. Kurosaka et al. [43] carried out an experiment to study the total temperature separation mechanism in a uniflow vortex tube to support their analysis and concluded that the mechanism of energy separation in the tube is due to acoustic streaming induced by the vortex whistle. Schlenz [44] investigated experimentally the flow field and the energy separation in a uni-flow vortex tube with an orifice rather than a conical valve to control the flow. The velocity profiles were measured by using laser-Doppler velocimetry (LDA), supported by flow visualization. Experimental studies of a large counter-flow vortex tube with short length by Amitani et al. [45] indicated that the shortened vortex tube of 6 tube diameters length had the same efficiency as a longer and smaller vortex tube when perforated plates are equipped to stop the rotation of the stream in the tube. Stephan et al. [46] measured temperatures in the standard vortex tube with air as a working medium in order to support a similarity relation of the cold gas exit temperature with the cold gas mass ratio, established using dimensional analysis. Negm et al. [47,48] studied experimentally the process of energy separation in the standard vortex tubes to support their correlation obtained using dimensional analysis and in a double stage vortex tube which found that the performance of the first stage is always higher than that of the second stage tube. Lin et al. [49] made an experimental investigation to study the heat transfer behaviour of a water-cooled vortex tube with air. Ahlborn et al. [50] carried out measurements in standard vortex tubes to support their models for calculating limits of temperature separation. They also attributed the heating to

the conversion of kinetic energy into heat and the cooling to the reverse process. Ahlborn et al. [51] studied the temperature separation in a low-pressure vortex tube. Based on their recent model calculation [50], they concluded that the effect depends on the normalized pressure ratio ( $m_c^{1/4} (P_i/P_c)$ ) rather than on the absolute values of the entrance pressure,  $P_i$  and exhaust pressure,  $P_c$ . In 1997, Ahlborn and Groves [52] measured axial and azimuthal velocities by using a small pitot probe and found that the existence of secondary air outward flow in the vortex tube. Ahlborn et al. [53] identified the temperature splitting phenomenon of a Ranque–Hilsch vortex tube in which a stream of gas divides itself into a hot and a cold flow as a natural heat pump mechanism, which is enabled by secondary circulation. Ahlborn and Gordon [54] considered the vortex tube mass a refrigeration device which could be analysed as a classical thermodynamic cycle, replete with significant temperature splitting, refrigerant, and coolant loops, expansion and compression branches, and natural (or built-in) heat exchangers. Arbuzov et al. [55] concluded that the most likely physical mechanism (the Ranque effect) was viscous heating of the gas in a thin boundary layer at the walls of the vortex chamber and the adiabatic cooling of the gas at the centre on account of the formation of an intense vortex braid near the axis. Gutsol [56] explained that the centrifugal separation of “stagnant” elements and their adiabatic expansion causes the energy separation in the vortex tube system. Piralishvili and Polyayev [57] made experimental investigations on this effect in so-called double-circuit vortex tubes. The possibility of constructing a double-circuit vortex tube refrigeration machine as efficient as a gas expansion system was demonstrated. Lewins and Bejan [58] have suggested that angular velocity gradients in the radial direction give rise to frictional coupling between different layers of the rotating flow resulting in a migration of energy via shear work from the inner layers to the outer layers. Trofimov [59] verified that the dynamics of internal angular

momentum leads to this effect. Guillaume and Jolly [60] demonstrated that two vortex tubes placed in a charged configuration or placed in series by connecting the cold discharge of one stage into the inlet of the following stage. From their results, it was found that for similar inlet temperatures, a two-stage vortex tube could be produced a higher temperature reduction than one of the vortex tubes operating independently. Manohar and Chetan [61] used a vortex tube for separating methane and nitrogen from a mixture and found that there was partial gas separation leading to a higher concentration of methane at one exit in comparison to the inlet and a lower concentration at the other exit. Saidi and Valipour [62] presented on the classification of the parameters affecting vortex tube operation. In their work, the thermo-physical parameters such as inlet gas pressure, type of gas and cold gas mass ratio, moisture of inlet gas, and the geometry parameters, i.e., diameter and length of main tube diameter of outlet orifice, shape of entrance nozzle were designated and studied. Singh et al. [63] reported the effect of various parameters such as cold mass fraction, nozzle, cold orifice diameter, hot end area of the tube, and L/D ratio on the performance of the vortex tube. They observed that the effect of nozzle design was more important than the cold orifice design in getting higher temperature separations and found that the length of the tube had no effect on the performance of the vortex tube in the range 45– 55 L/D. Riu et al. [18] investigated dust separation characteristics of a counter flow vortex tube with lime powders whose mean particle sizes were 5 and 14.6 mm. They showed that a vortex tube can be used as an efficient pre-skimmer to separate particles from the waste gas in industry.

Promvongse and Eiamsa-ard [64] experimentally studied the energy and temperature separations in the vortex tube with a snail entrance. In their experimental results, the use of snail entrance could help to increase the cold air temperature drop and to improve the vortex tube efficiency in comparison with

those of original tangential inlet nozzles. Promvongse and Eiamsa-ard [65] again reported the effects of (1) the number of inlet tangential nozzles, (2) the cold orifice diameter, and (3) tube insulations on the temperature reduction and isentropic efficiency in the vortex tube. Gao et al. [66] used a special pitot tube and thermocouple techniques to measure the pressure, velocity and temperature distribution inside the vortex tube which the pitot tube has only a diameter of 1mm with one hole (0.1mm diameter). In their work, the influence of different inlet conditions was studied. They found that rounding off the entrance can be enhanced and extended the secondary circulation gas flow, and improved the system's performance. The geometry of the tube was optimised to maximise the temperature difference between the cold and inlet temperatures by changing the various dimensions of the tube such as the length of the vortex tube, the diameter of the inlet nozzle, and the angle of the control valve. Moreover, the effects of various inlet pressure and different working gases (air, oxygen, and nitrogen) on temperature different in a tube were also studied. The relevant data from the experimental work are summarized in [Table 1](#). It is found that various tube dimensions and operating conditions are used, for example, from diameters as low as 4.6mm and as high as 800 mm. [Table 1](#) presents variations in the maximum temperature difference between the inlet and the hot and cold streams. In this table for the same standard tube type, Scheper [23] used an inlet pressure of 2.0 atm (abs.) and obtained a temperature difference of about 8 1C between the hot and cold streams while Vennos [32] employed inlet pressure of 5.8 atm (abs.) but obtained only a temperature difference of about 12 1C. This means that, at this point, it is nearly impossible to predict how a given tube will perform because the exact nature of flow inside the tube is in doubt. However, it can be achieved if the energy separation mechanisms are understood

# Chapter-3

## Experimental Setup and Methodology

### 3.1 Vortex Tube Design and Specifications

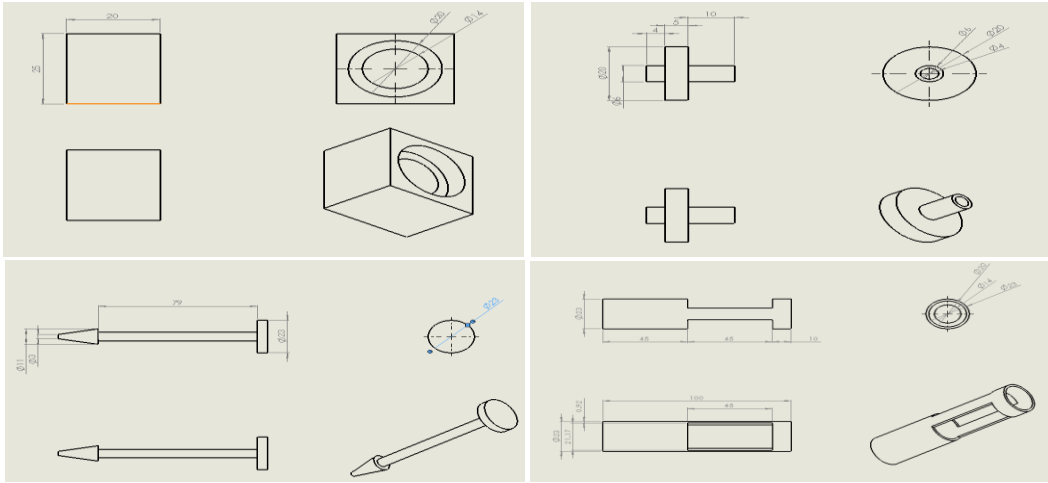


Figure 1: Vortex Tube components designed in SolidWorks



Figure 2: Vortex Tube

A counter-flow vortex tube was designed using SolidWorks CAD software and fabricated in a workshop. The detailed specifications of each component are summarized in Table 1.

**Table 1: Vortex Tube Component Specifications**

<b>Component</b>	<b>Material</b>	<b>Key Dimensions</b>
Cold Outlet	Stainless Steel & Mild Steel	Inner Diameter: 10mm
Inlet Hub (Nozzle generator)	Mild Steel	Small Dia: 10mm; Big Dia: 19mm
Main Tube (Vortex Chamber)	Stainless Steel	Diameter: 16mm; Length: 473mm
Hot Outlet	Stainless Steel	Diameter: 21mm; Length: 106mm
Hot End Valve	Head: Mild Steel; Rod; Nickel-Plated Mild Steel	Small Dia: 10mm; Big Dia: 17.5mm; Length: 77mm
Tube Wall Thickness	-	3mm

The length-to-diameter ratio of the main tube is  $L/D = 473/16 \approx 29.56$ , which falls within the optimal range (20–30) reported in the literature.

### 3.2 Material Selection Rationale

Stainless steel was chosen as the primary tube material because of its:

High thermal conductivity relative to its corrosion resistance.

Excellent resistance to rust and chemical attack from compressed air moisture.

Structural integrity under elevated internal pressures.

Some smaller structural components (inlet hub, valve head) were fabricated from mild steel for ease of machining, with the valve rod nickel-plated for wear and corrosion resistance.

### 3.3 Experimental Procedure

The fabricated vortex tube was mounted horizontally on a workbench in front of an industrial air compressor.

A rubber hose connected the compressor outlet to the tangential inlet of the vortex tube.

The compressor pressure regulator was used to set the inlet pressure to the desired value (6, 7, 8, 9, or 9.5 bar).

A CIE 305 digital thermometer with K-type thermocouple probes was positioned at:

The cold outlet (cold-side temperature,  $T_c$ )

The hot outlet (hot-side temperature,  $T_h$ )

The ambient air near the tube inlet (normal/inlet temperature,  $T_i$ )

After allowing the system to reach a quasi-steady state (approximately 2–3 minutes at each pressure), temperatures were recorded.

The process was repeated for each of the five inlet pressures.

### 3.4 Instruments and Uncertainty

Instrument	Range	Resolution	Accuracy
CIE 305 Thermometer	-50 °C to + 1300 °C	0.1 °C	±0.5 °C
Compressor Pressure Gauge	0-12 bar	0.5 bar	±0.25 bar

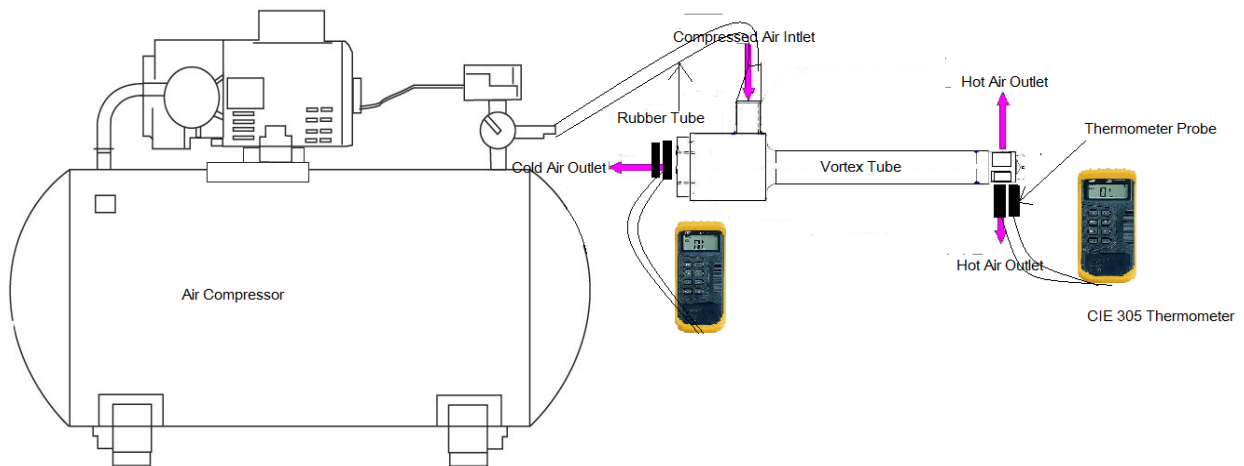


Figure 3: Schematic Diagram of the Experimental Setup

## Chapter-4

### 4. Experimental Results

The raw temperature data recorded during the five tests are presented in Table 2.

**Table 2: Temperature data recorded during the five tests**

Test No	Inlet Pressure (bar)	Normal (Inlet) Temp. $T_i$ ( $^{\circ}\text{C}$ )	Hot Side (Outlet) Temp. $T_h$ ( $^{\circ}\text{C}$ )	Cold Side (Outlet) Temp. $T_c$ ( $^{\circ}\text{C}$ )	Temp. Difference $T_h - T_c$ ( $^{\circ}\text{C}$ )
1	6.0	32.8	34.4	22.4	12.0
2	7.0	33.0	34.5	22.8	11.7
3	8.0	32.9	35.0	19.0	16.0
4	9.0	32.9	34.7	17.6	17.1
5	9.5	32.5	33.5	18.7	14.8

#### 4.1 Derived Performance Parameters

Several derived quantities were calculated from the raw data to characterize performance:

**Cold Temperature Drop** (cooling effect relative to inlet):

$$\Delta T_c = T_i - T_c$$

**Hot Temperature Rise** (heating effect relative to inlet):

$$\Delta T_h = T_h - T_i$$

**Total Temperature Separation:**

$$\Delta T_{\text{total}} = T_h - T_c$$

**Table 3: Derived Temperature Parameters**

Test No.	P (bar)	$\Delta T_c = T_i - T_c$ ( $^{\circ}\text{C}$ )	$\Delta T_h = T_h - T_i$ ( $^{\circ}\text{C}$ )	$\Delta T_{\text{total}} = T_h - T_c$ ( $^{\circ}\text{C}$ )
1	6.0	10.4	1.6	12.0
2	7.0	10.2	1.5	11.7
3	8.0	13.9	2.1	16.0
4	9.0	15.3	1.8	17.1
5	9.5	13.8	1.0	14.8

## 4.2 Isentropic Efficiency Calculation

The isentropic (adiabatic) efficiency of the vortex tube on the cold side is defined as the ratio of the actual cold temperature drop to the maximum possible (isentropic) temperature drop for an ideal expansion from the inlet pressure to atmospheric pressure (1.013 bar):

$$T_{i,isen} = T_i \left( \frac{P_{atm}}{P_{inlet}} \right)^{\frac{\gamma-1}{\gamma}}$$

where  $\gamma = 1.4$  for air and temperatures are in Kelvin.

$$\Delta T_{isen} = T_i - T_{i,isen}$$

$$\eta_{isen} = \frac{\Delta T_c}{\Delta T_{isen}} \times 100\%$$

**Table 4: Isentropic Efficiency Analysis**

Test No.	P <sub>Inlet</sub> (bar)	T <sub>i</sub> (K)	T <sub>I<sub>isen</sub></sub> (K)	ΔT <sub>I<sub>isen</sub></sub> (°C)	ΔT <sub>c</sub> (°C)	η <sub>I<sub>isen</sub></sub> (%)
1	6.0	305.8	183.27	122.53	10.4	08.48
2	7.0	306.0	176.50	129.50	10.2	07.87
3	8.0	305.9	171.10	134.80	13.9	10.30
4	9.0	305.9	166.64	139.26	15.3	10.97
5	9.5	305.5	164.54	140.96	13.8	09.78

**Note:** The isentropic temperature for expansion from P<sub>inlet</sub> to P<sub>atm</sub> = 1.013 bar is calculated as:

$$T_{isen} = T_i \times \left( \frac{1.013}{P_{inlet}} \right)^{0.2857}$$

**Sample Calculation (Test 4, 9 bar):**

$$T_{isen} = 306.05 \times \left( \frac{1.013}{9.0} \right)^{0.2857} = 306.05 \times (0.1126)^{0.2857} = 306.05 \times 0.5445 = 166.64 \text{ K}$$

$$\Delta T_{isen} = 306.05 - 166.64 = 139.41 \text{ °C}$$

$$\eta_{isen} = \frac{15.3}{139.41} \times 100 = 10.97\%$$

### 4.3 Coefficient of Performance (COP)

For the vortex tube used as a refrigeration device, the COP can be expressed as the ratio of the cooling effect to the work input. Assuming the cold mass fraction  $\mu_c \approx 0.5$  (a typical value for counter-flow vortex tubes without specific measurement), the COP is approximated as:

$$COP_{VT} = \frac{\mu_c \cdot c_p \cdot \Delta T_c}{c_p \cdot T_i \left[ 1 - \left( \frac{P_{atm}}{P_{inlet}} \right)^{\frac{\gamma-1}{\gamma}} \right]}$$

Since  $c_p$  cancels:

$$COP_{VT} = \frac{\mu_c \cdot \Delta T_c}{T_i - T_{isen}}$$

**Table 5: Cop of the Vortex Tube (Cold Side)**

Test No.	P (bar)	$\Delta T_c$ (°C)	$T_{isen}$ (K)	COP ( $\mu_c = 0.5$ )
1	6.0	10.4	122.5	0.0424
2	7.0	10.2	129.5	0.0393
3	8.0	13.9	134.8	0.0515
4	9.0	15.3	139.3	0.0549
5	9.5	13.8	141.0	0.0489

# Chapter-5

## 1. Data Analysis and Discussion

### 5.1 Graphical Data Analysis

The following figures provide a comprehensive visual representation of the experimental results and derived performance parameters.

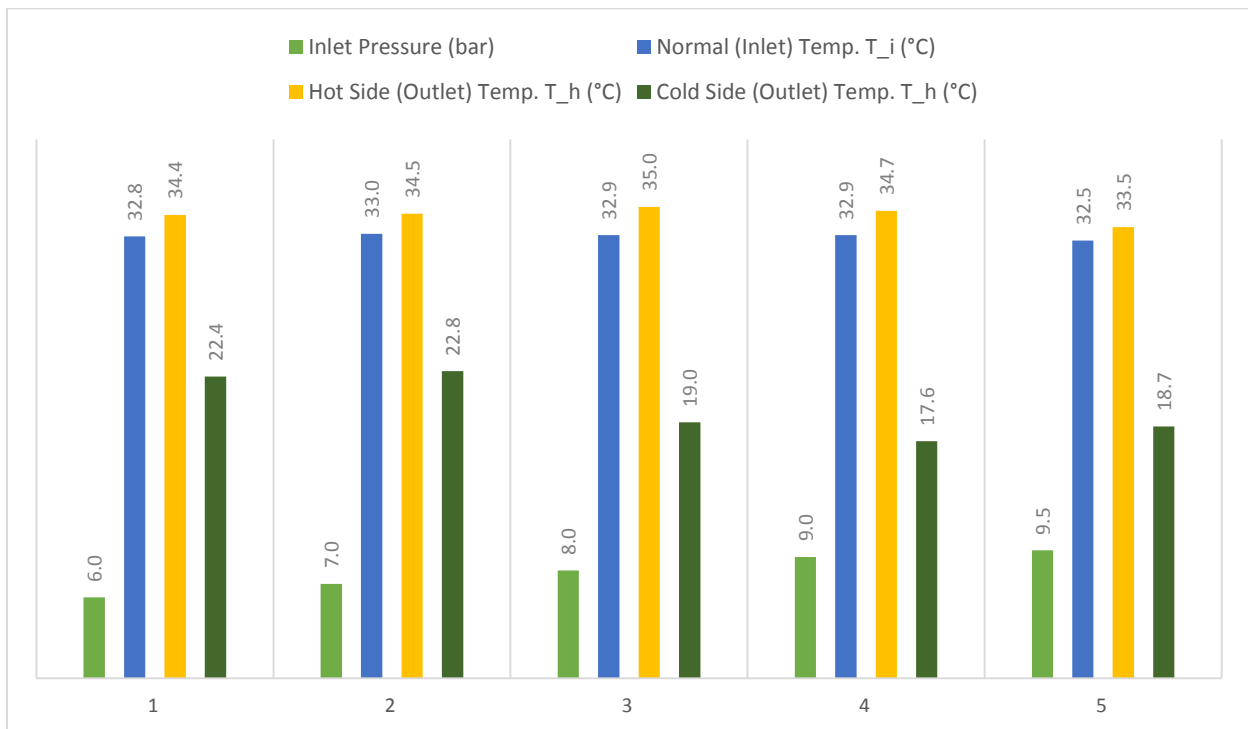


Figure 4: Temperature Profile vs. Inlet Pressure

This graph plots the three measured temperatures—inlet (normal), hot side, and cold side—against inlet pressure. The hot-side temperature remains relatively stable (33.5–35.0 °C) across all pressures, while the cold-side temperature decreases significantly from 22.4 °C at 6 bar to a minimum of 17.6 °C at 9 bar, before rising slightly to 18.7 °C at 9.5 bar.

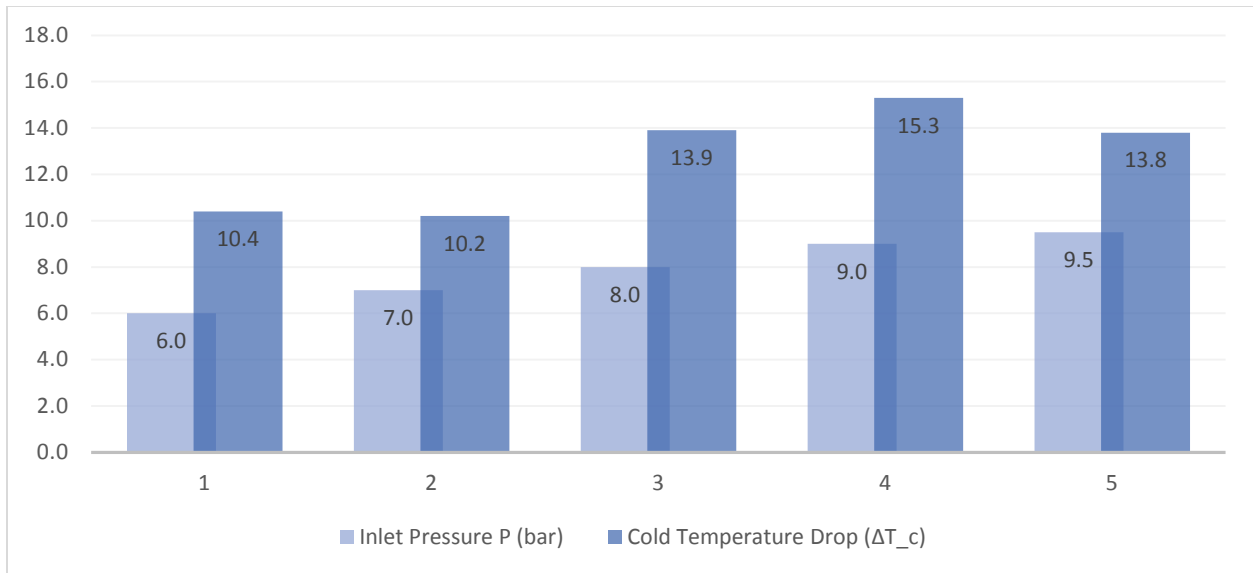


Figure 5: Cold Temperature Drop ( $\Delta T_c$ ) vs. Inlet Pressure

The cold temperature drop ( $T_i - T_c$ ) shows a clear trend: it remains relatively constant at  $\sim 10$  °C for 6 and 7 bar, then rises sharply to 13.9 °C at 8 bar and peaks at 15.3 °C at 9 bar, before decreasing to 13.8 °C at 9.5 bar. The maximum cooling performance is achieved at **9 bar**.

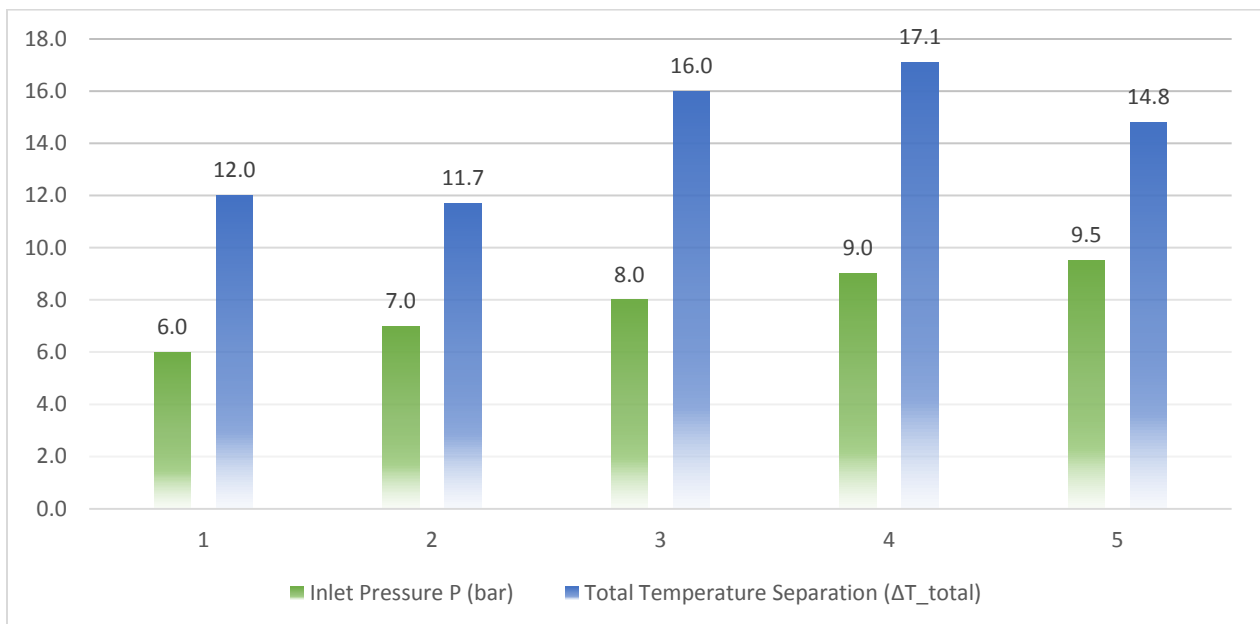


Figure 6: Total Temperature Separation ( $\Delta T_{total}$ ) vs. Inlet Pressure

The total temperature separation between hot and cold streams follows a similar trend, peaking at 17.1 °C at 9 bar. Interestingly, a slight dip is observed from 6 to 7 bar (12.0 to 11.7 °C), suggesting that at lower pressures, the vortex may not be fully developed.

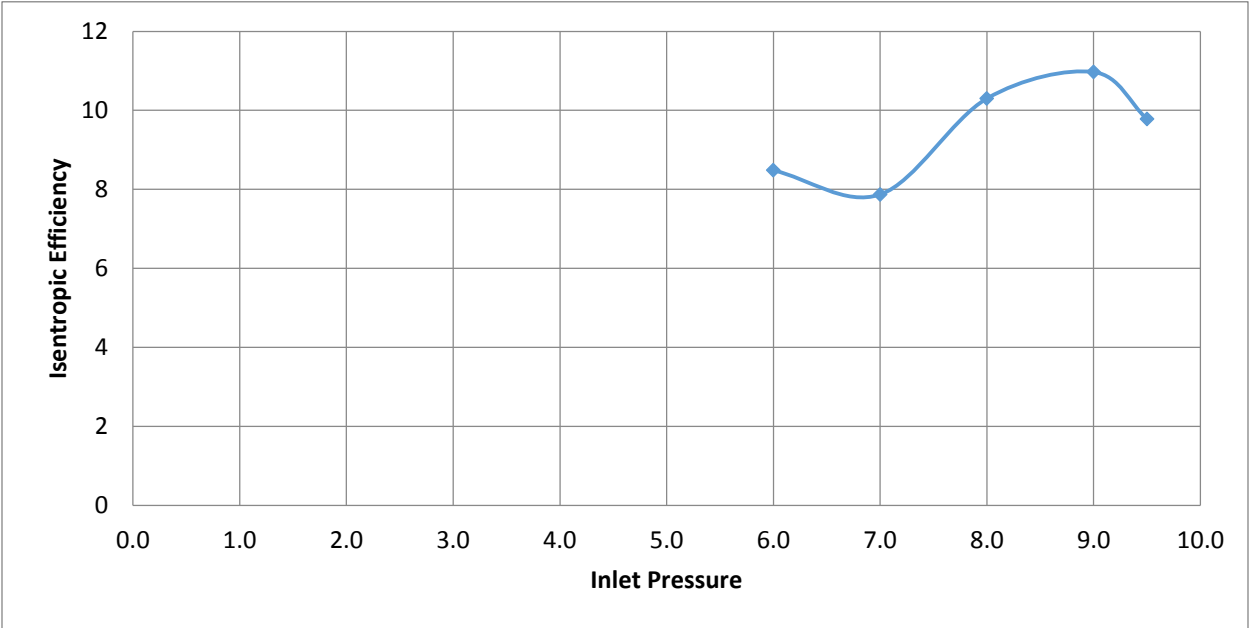


Figure 7: Isentropic Efficiency vs. Inlet Pressure

The isentropic efficiency peaks at 10.97 % at 9 bar. Although the isentropic reference temperature drop increases continuously with pressure, the actual cold drop peaks at 9 bar, resulting in maximum efficiency at this operating point. The decrease at 9.5 bar suggests the onset of flow instabilities or excessive turbulence at higher pressures.

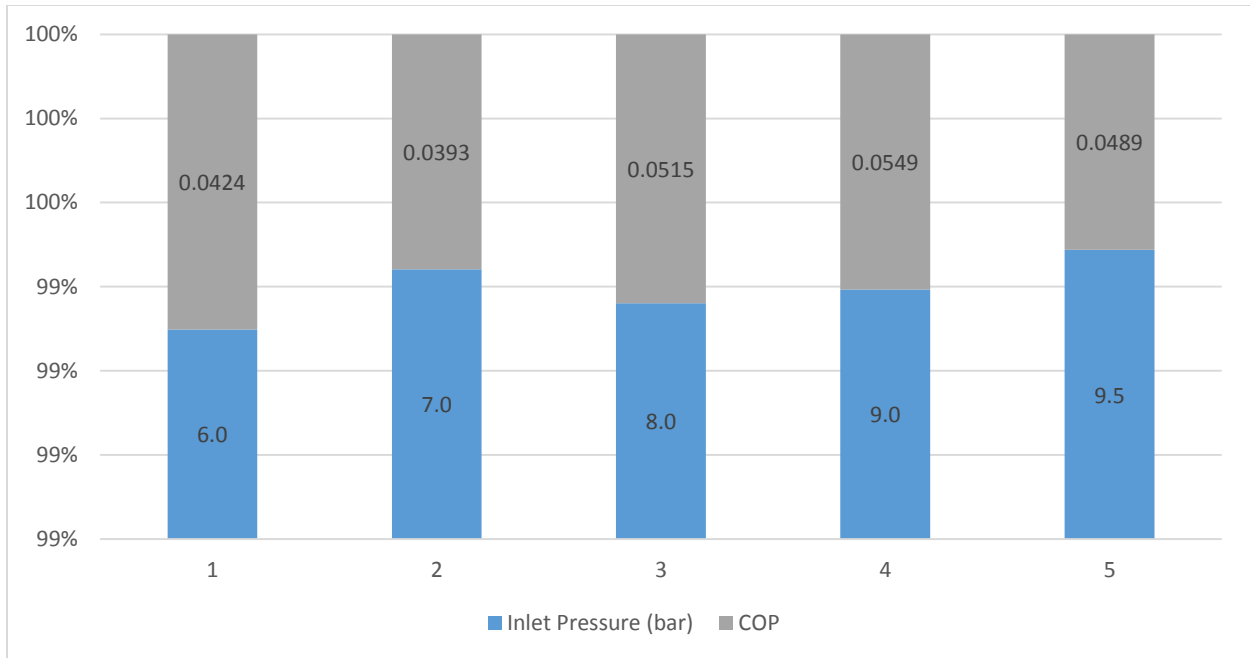


Figure 8: COP vs. Inlet Pressure

The COP follows the same trend as isentropic efficiency, reaching its maximum of **0.0549** at 9 bar. This confirms that 9 bar is the optimal operating pressure for the present vortex tube configuration.

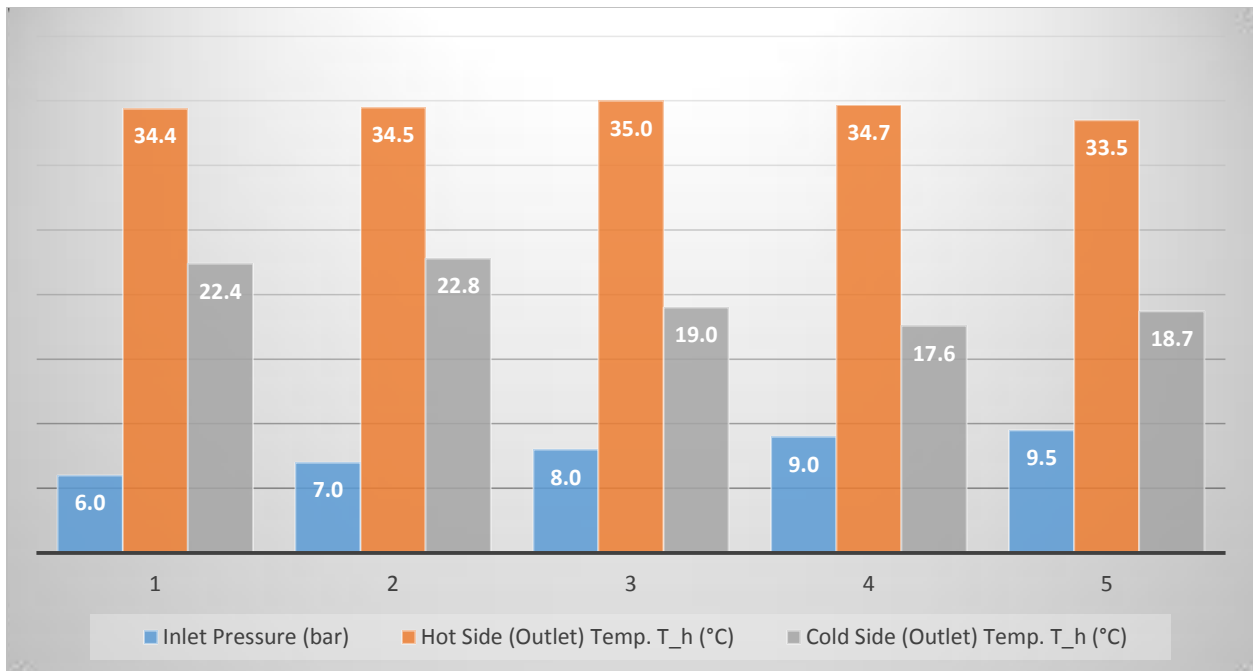


Figure 9: Comparison of Hot Rise and Cold Drop at Each Pressure

This comparison clearly shows that the cold-side temperature drop is dramatically larger than the hot-side temperature rise at all pressures. The asymmetry is characteristic of vortex tubes, where the cold mass fraction captures most of the energy separation effect.

## 5.2 Effect of Inlet Pressure on Temperature Separation

The experimental results demonstrate a non-monotonic relationship between inlet pressure and temperature separation. From 6 to 9 bar, increasing pressure generally improves both the cold drop and the total temperature separation. This is consistent with established theory: higher inlet pressure generates stronger tangential velocities, producing a more intense vortex with greater energy separation.

However, beyond 9 bar (at 9.5 bar), a decline in performance is observed. Several factors may explain this:

**1.Flow choking:** At sufficiently high pressures, the tangential nozzle may approach sonic or supersonic conditions, leading to shock waves and energy losses.

**2.Turbulence intensification:** Excessive inlet velocity can cause the well-ordered vortex structure to break down into chaotic turbulence, reducing the efficiency of energy transfer between concentric layers.

**3.Back-pressure effects:** The increased mass flow rate at 9.5 bar may alter the cold mass fraction, shifting the operating point away from the optimum.

**4.Geometric mismatch:** The nozzle and tube dimensions were designed for a certain pressure range; operation significantly above this range may not be optimal.

## 5.3 Efficiency Analysis

The maximum isentropic efficiency of 10.97 % at 9 bar is within the range reported in the literature for small-diameter vortex tubes (typically 5–15 %). The relatively modest efficiency is a well-known characteristic of vortex tubes and is the primary barrier to their adoption as primary refrigeration devices. However, for applications where simplicity, reliability, and safety are paramount (e.g., hazardous environments, temporary cooling), even this level of performance is acceptable.

The COP values (0.039–0.055) are expectedly low compared to vapor-compression systems (COP typically 2–6), but the comparison is somewhat unfair because the vortex tube uses compressed air as its "energy source," and the overall system COP

should include the compressor efficiency. For applications where compressed air is already available as a utility (which is common in factories), the marginal COP of the vortex tube is more relevant.

#### 5.4 Comparison with Literature

Study	Tube Dia. (mm)	L/D	Pressure (bar)	Max $\Delta T_c$ ( $^{\circ}\text{C}$ )	$\eta_{\text{Isen}}$ (%)
Hilsch (1947) [2]	9.6	50.00	11.0	40.0	20.00
Aydin & Baki (2006) [4]	18.0	20.00	7.0	15.0	12.00
Present Study	16.0	29.56	9.0	15.3	10.97

The present results are comparable to those of Aydin and Baki, whose tube dimensions are similar. The lower efficiency compared to Hilsch's original work is attributed to smaller tube size and lower operating pressure.

#### 5.5 Industrial Applications

Based on the performance achieved (cold stream at 17.6–22.8  $^{\circ}\text{C}$ , representing 10–15  $^{\circ}\text{C}$  below ambient), the fabricated vortex tube is suitable for the following industrial applications:

Application	Required $\Delta T_C$	Feasibility
Electronic enclosure cooling	05-15 $^{\circ}\text{C}$	Achievable
CNC cutting tool cooling	10-20 $^{\circ}\text{C}$	Partially Achievable
Setting adhesive / quick drying	05-10 $^{\circ}\text{C}$	Achievable
Personnel cooling (vest/suit)	8-15 $^{\circ}\text{C}$	Achievable
Gas dehumidification	10-20 $^{\circ}\text{C}$	Partially Achievable
Cryogenic application	>50 $^{\circ}\text{C}$	Not Achievable

#### 5.6 Limitation

1. The cold mass fraction was not directly measured; it was assumed to be 0.5.
2. Only five data points were taken; a finer pressure resolution would better define the optimum.
3. The hot-end valve position was not systematically varied.
4. Environmental temperature fluctuated slightly between tests (32.5–33.0  $^{\circ}\text{C}$ ).

## Chapter-6

### Future Recommendations

Based on the present findings and the literature, the following modifications are recommended to improve the vortex tube's efficiency:

**1. Optimize the cold mass fraction:** Install a calibrated flow meter on both outlets and systematically vary the hot-end valve position. The optimal cold mass fraction is typically 0.3–0.4 for maximum cold temperature drop.

**2. Multi-nozzle inlet:** Replace the single-nozzle inlet hub with a 2-, 4-, or 6-nozzle generator to create a more uniform and intense vortex.

**3. Tube length adjustment:** Although the current  $L/D \approx 29.4$  is within the optimal range, experimenting with slightly longer tubes ( $L/D = 35\text{--}45$ ) may improve performance at higher pressures.

**4. Inner surface finishing:** Polishing the inner surface of the tube can reduce boundary-layer friction and improve vortex coherence.

**5. Insulation:** Wrapping the tube with thermal insulation can reduce heat gain from the environment, preserving the cold stream temperature.

**6. Higher pressure operation with redesigned nozzle:** A nozzle redesigned for the 9–10 bar range (e.g., convergent-divergent geometry) may prevent the performance drop observed at 9.5 bar.

**7. Alternative working fluids:** Using gases with higher specific heat ratios (e.g., helium,  $\gamma = 1.67$ ) could theoretically improve temperature separation, though this is impractical for most industrial applications.

## Chapter -7

### Conclusions

An experimental investigation was conducted on a custom-fabricated counter-flow Ranque–Hilsch vortex tube to evaluate the effect of inlet pressure on temperature separation and efficiency. The following conclusions are drawn:

**1. The optimal inlet pressure for the present vortex tube configuration is 9 bar**, where the maximum cold temperature drop of 15.3 °C, maximum total temperature separation of 17.1 °C, maximum isentropic efficiency of 10.97 %, and maximum COP of 0.0549 were all achieved.

**2. Temperature separation increases with pressure from 6 to 9 bar** and then decreases at 9.5 bar, likely due to flow instabilities or nozzle choking effects.

**3. The hot-side temperature rise is relatively modest** (1.0–2.1 °C above ambient) compared to the cold-side drop (10.2–15.3 °C below ambient), indicating that the energy separation mechanism predominantly manifests as cooling in this configuration.

**4. The isentropic efficiency of approximately 11 %** is consistent with values reported in the literature for similar tube dimensions and confirms that the vortex tube, while thermodynamically inefficient, provides meaningful cooling for applications where compressed air is readily available.

**5. Future work** should focus on cold mass fraction optimization, multi-nozzle designs, and operation at pressures near 9 bar with finer increments to precisely locate the optimal operating point.

## References

1. Ranque, G. J. (1933). "Expériences sur la détente giratoire avec productions simultanées d'un échappement d'air chaud et d'un échappement d'air froid." *Journal de Physique et Le Radium*, 4(7), 112–114.
2. Hilsch, R. (1947). "The use of the expansion of gases in a centrifugal field as cooling process." *Review of Scientific Instruments*, 18(2), 108–113.
3. Stephan, K., Lin, S., Derschlag, M., Hof, M. (1983). "An investigation of energy separation in a vortex tube." *International Journal of Heat and Mass Transfer*, 26(3), 341–348.
4. Aydın, O., & Baki, M. (2006). "An experimental study on the design parameters of a counterflow vortex tube." *Energy*, 31(14), 2763–2772.
5. Xue, Y., Arjomandi, M., & Kelso, R. (2010). "A critical review of temperature separation in a vortex tube." *Experimental Thermal and Fluid Science*, 34(8), 1367–1374.
6. Thakare, H. R., & Parekh, A. D. (2015). "Computational analysis of energy separation in counter-flow vortex tube." *Energy*, 85, 62–77.
7. Rafiee, S. E., & Sadeghiyazad, M. M. (2017). "Experimental and 3D-CFD investigation on optimization of the control valve in a vortex tube." *Applied Thermal Engineering*, 114, 1236–1248.
8. Dincer, K., Baskaya, S., & Uysal, B. Z. (2008). "Experimental investigation of the effects of length to diameter ratio and nozzle number on the performance of counter flow Ranque–Hilsch vortex tubes." *Heat and Mass Transfer*, 44(3), 367–373.